

## Resonance modes and gap formation in a two-dimensional solid phononic crystal

Honggang Zhao,\* Yaozong Liu, Gang Wang, Jihong Wen, Dianlong Yu, Xiaoyun Han, and Xisen Wen  
*Institute of Mechatronic Engineering, and PBG Research Center, National University of Defense Technology,  
 Changsha 410073, China*

(Received 5 December 2004; revised manuscript received 4 March 2005; published 7 July 2005)

The resonance modes near the edges of the first absolute band gap of a two-dimensional solid phononic crystal with an epoxy host are investigated in this paper. A rotary resonance mode, induced by the joint effect of the Bragg and Mie scattering, is observed near the bottom of the gap. The gap, resulting from the interaction between the rigid-body resonance and the effective homogeneous medium, coalesces with the Bragg gap, which leads to the formation of a wide gap. Then a simple analytical model is introduced to give a physically intuitive account of the rotary resonance. Finally, the effects of the array and the filling fraction on the band gap are explained by the conditions for occurrence of the resonance.

DOI: [10.1103/PhysRevB.72.012301](https://doi.org/10.1103/PhysRevB.72.012301)

PACS number(s): 46.40.-f, 43.20.+g, 43.40.+s

A phononic crystal (PC) is a composite material whose density and/or elastic coefficients vary periodically in space.<sup>1</sup> Under certain conditions, PCs can exhibit a phononic band gap (PBG). The PBG is a frequency domain where the propagation of the elastic wave is forbidden. Further to Sigalas's structural proposal,<sup>2</sup> the band gaps and the mathematical analogy between the elastic waves in PCs and electromagnetic waves in photonic crystals<sup>3</sup> have been extensively studied during the last decade.<sup>4-13</sup> Most of these studies focused on identifying the absolute band gaps in various PCs.<sup>4-7</sup> For a solid-solid system, the absolute gap is difficult to find because the longitudinal and transverse waves are mixed. The contrast between the elastic coefficients and densities of the compositions of the PC is critical in determining the existence and the width of the PBG (reviewed by Kafesaki<sup>6</sup>). As for the formation of the gap, Sainidou *et al.* showed in three-dimensional (3D) PCs (steel spheres in polyester) that the gap originates from the interaction between the rigid-body resonance (RBR) of the individual sphere and the effective homogeneous medium.<sup>7</sup> Maslov studied the RBR theoretically and the lattice resonance experimentally.<sup>8</sup> In this paper, we give further investigation of the resonance modes and the formation of the gap.

We choose a two-dimensional solid-solid PC, which permits the propagation of the pure transverse ( $Z$  mode) and the mixed modes ( $XY$  mode) independently when restricting the wave vector  $\vec{k}$  propagating in the  $XY$  plane (see Fig. 1). We confine our attention to the  $XY$  mode. Compared to 3D PCs, there is one less transverse mode mixed in the  $XY$  mode, which simplifies the nature of the eigenmodes and the corresponding computation, and makes it easier to understand the physical origin of the gaps.

First, a square array of glass cylinders with circular cross section in epoxy is considered (for material parameters see Table I). The geometry is illustrated in Fig. 1. Figure 2(a) shows the band structure calculated by the improved plane-wave expansion (IPWE) method.<sup>9</sup> The filling fraction  $F$  is 0.45 and 441 plane waves are used in this and the following calculations. The frequencies are normalized as  $fa/c_t$ , where  $c_t$  is the transverse wave velocity in epoxy. From Fig. 2(a), we can see that the first absolute PBG exists between the

third and fourth bands. The long-wavelength limit ( $f \rightarrow 0$ ) presents two linear dispersion curves (corresponding to the transverse and the longitudinal waves propagating in the PC, respectively), the slopes of which give the effective velocities of the composite medium. Here the PC behaves as a homogenous medium. Figure 3(a) shows the particle displacement vectors calculated by the lumped-mass method.<sup>10</sup> It can be seen that all the particles in the lattice move in phase and with the same amplitude. The particle displacement vectors at the gap bottom ( $\Gamma$  point denoted by  $B$ ) are showed in Fig. 3(b). The distinct feature is the standing wave accompanied by a rotary resonance, i.e., the glass rod revolves about its axis and the epoxy vibrates accordingly. This resonance mode is induced by the joint effect of the Bragg and Mie scattering. The former originates from the lattice periodicity and the contrast between the material parameters of the components. The periodicity makes the linear dispersion of the effective homogeneous medium fold onto the first Brillouin zone. This effect can be explained in the case that there is little contrast between the material parameters of the components. Generally, a small or no gap will be opened. In the glass-epoxy system, the contrast of the acoustic impedance, i.e., the product of the density and the velocity, induces reflection between the adjacent layers along a specific direction. This reflection is enhanced when the transmitting distance of the reflective waves from adjacent layers meets the corresponding wavelength, which leads to zero transmission

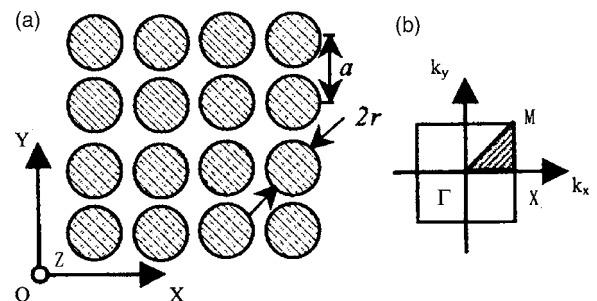


FIG. 1. (a) Cross section of the two-dimensional square array of glass cylinders with radius  $r$  in epoxy.  $a$  is the lattice constant. (b) The high-symmetry points  $\Gamma$ ,  $X$ , and  $M$  in the first Brillouin zone.

TABLE I. Parameters of the materials employed in this paper.

Material	$\rho$ (kgm <sup>-3</sup> )	$c_l$ (ms <sup>-1</sup> )	$c_t$ (ms <sup>-1</sup> )
Glass	2490	5660	3300
Al	2690	6450	3220
Al <sub>2</sub> O <sub>3</sub>	3970	10850	6345
BaCO <sub>3</sub>	5300	5170	2780
Steel	7890	5780	3220
Cu	8960	4330	2900
W	19300	5090	2800
Au	19500	3360	1239
Epoxy	1220	2490	1180

in the specific frequency range. This is the physical origin of the Bragg gap. This gap will be dependent on the symmetry of the lattice, the bottom of the gap is mainly determined by the wave scattering along the  $[1,0]$  direction, and its top is mainly determined by the wave scattering along the  $[1,1]$  direction. As a verification, Fig. 3(d) shows the particle displacement vectors at the gap top [denoted by point  $D$  in Fig. 2(a)]. On the other hand, the weak RBR of the individual cylinder, resulting from the Mie scattering, exists near the bottom of the Bragg gap. Figure 3(c) shows the particle displacement vectors [denoted by the line with arrowhead at point  $C$  in Fig. 2(a)]. A series of such resonators attach to and interact with the effective homogeneous medium, which leads to zeros of transmission in the gap (PCs with a locally resonant structure serve as good examples for understanding the formation mechanism of the gap<sup>11-13</sup>). This gap coalesces with the Bragg gap, so a wider gap comes into being.

In order to support the origin of the wide gap stated above, the resonance modes of various cylinder materials with larger densities are also investigated (for material parameters see Table I). The results show that the particle displacement vectors present almost the same patterns as the glass-epoxy system at the corresponding point. The main difference is that a greater rotary resonance exists near the gap bottom as the cylinder density is getting larger. As we know,

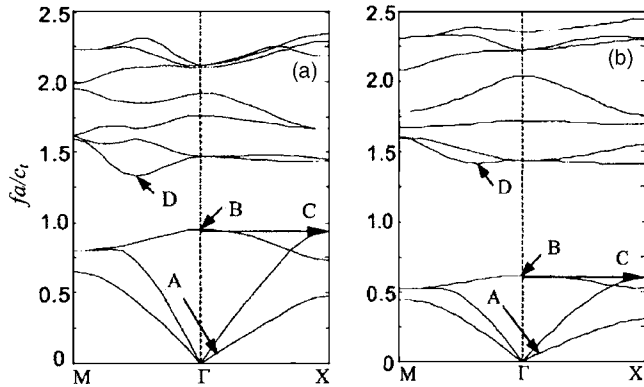


FIG. 2. Dispersion relations of XY modes in 2D (a) glass-epoxy and (b) steel-epoxy with square array.  $F=0.45$ . A, linear dispersion area; B and D, bottom edge and top edge of the first absolute PBG, respectively; C, the band of RBR mode.

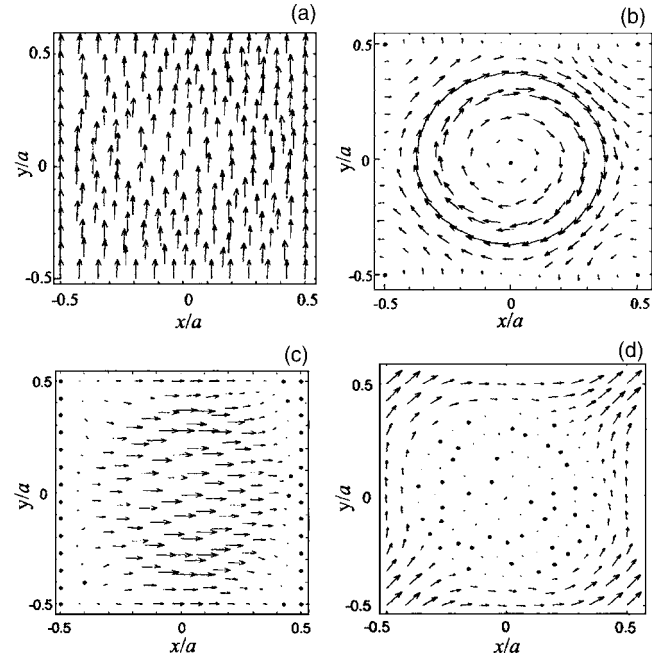


FIG. 3. Particle displacement vectors of XY mode  $u_{xy}$  in one unit cell. The direction and length of the arrows represent the direction and amplitude of the displacement vectors, respectively. The selected wave vector and frequency are corresponding to point (a) A, (b) B, (c) C, and (d) D in Fig. 2, respectively.

the intensity of RBR increases with increase of the cylinder density (it behaves very similarly as in 3D systems<sup>8</sup>), which is denoted by the relatively flatter band. As can be seen from the steel-epoxy system in Fig. 2(b). At the same time, the frequency of RBR gets lower, so the gap induced by the RBR exists in the lower-frequency domain, and widens the corresponding Bragg gap too.

Now, we introduce a simple model for more physical insight into the rotary resonance. When  $F$  is lower or a little higher than 0.43 (0.47) in the square (triangular) array, the cylinders can rotate almost freely. So the resonant frequency can be estimated from a single cylinder in one unit cell. The rotary inertia of matrices with radii between  $R=r/a$  and  $1/2$  (the limit of the cylinder radii) is considered, which is reasonable according to the resonance pattern in Fig. 3(b). The rotary inertia  $I$  with unit length is

$$I = \pi \rho_s R^4 / 2 + \pi \rho_M [(3/2 - \sqrt{F/\pi})^4 - 1] R^4 / 2, \quad (1)$$

where  $\rho_s$  ( $\rho_M$ ) is the density of the cylinder (matrix). The corresponding effective torsional stiffness  $K_\theta$  is

$$K_\theta = 2\pi R^2 (\lambda_M + \mu_M), \quad (2)$$

where  $\lambda_M$  and  $\mu_M$  are the Lamé coefficients of the matrix. So the resonant frequency  $f$  is

$$f = \frac{1}{2\pi} \sqrt{K_\theta / I}. \quad (3)$$

Figure 4 shows the gap bottom as a function of the cylinder's density. The thick dash-dotted line represents the calculation result from (3). The thin solid line shows the gap

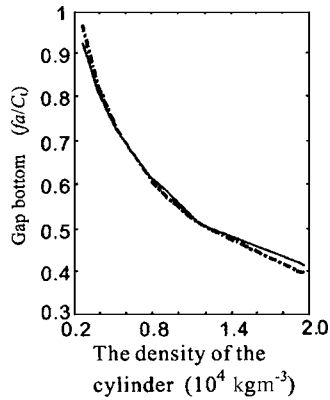


FIG. 4. The gap bottom as a function of the cylinder's density. The thick dash-dotted line represents the result by Eq. (3). The thin solid line shows the gap bottoms of various cylinder materials: glass, Al,  $\text{Al}_2\text{O}_3$ ,  $\text{BaCO}_3$ , steel, Cu, W, and Au in epoxy with a square array calculated with the IPWE,  $F=0.45$ .

bottoms of the PCs with various cylinder materials (for material parameters see Table I), which are calculated by the IPWE method. The good fittings show that the model is valid. It should be pointed out that the error between the result of the IPWE and that of Eq. (3) becomes more distinguishable when the cylinder's density is larger, which is induced by the convergence problem of the IPWE.

In this section, we will explain the effects of the array and the filling fraction on the first absolute PBG by the conditions for the resonance occurring. Figure 5 shows the variation of the gap edges (a) and width (b) of the steel-epoxy system with  $F$ . Let us look at the bottom of the gap first. When  $F \leq 0.43$  (0.47) in a square (triangular) array, the resonant frequency gets lower with increasing  $F$ , which is induced by the rotary inertia of the cylinder. It also can be seen from Fig. 5(a) that the gap bottom in the square array is lower than that of the triangular array. The reason is that there is a larger rotary inertia in the square array because of the larger radii under the same  $F$  ( $R = \sqrt{F/\pi}$  for the square array and  $\sqrt{3F/2\pi}$  for the triangular array). For  $F > 0.43$  (0.47) in the square (triangular) array, the stress from the neighbor cylinders, as a resistance, weakens the cylinder's rotation resonance. As a result, the interaction between the resonant cylinder and the matrix becomes weaker. Thus the frequency of the gap bottom gets higher. It is noticeable that the gap bottom of the square array is higher than that of the triangular array when  $F > 0.653$ , which is induced by the larger resistance in the square array under the same  $F$ .

Finally, the gap top is mainly determined by the Bragg scattering along the  $[1,1]$  direction, which leads to the gap

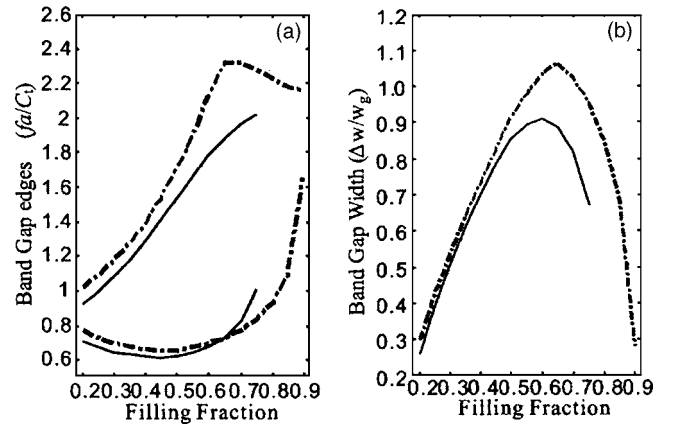


FIG. 5. The gap edges (a) and width (b) of the first absolute PBG in steel-epoxy system as a function of the filling fraction. Square array is represented by thin solid line and triangular array by thick dash-dotted line, respectively.

top of the triangular array is higher than that of the square array [Fig. 5(a)], so the band gap of the triangular array is wider than that of the square array under the same  $F$  [Fig. 5(b)]. For  $F \leq 0.57$  (0.65) in square (triangular) array, the distance between the boundaries of the neighbor cylinders is reduced while  $F$  increases; accordingly the wavelength of the standing wave becomes shorter, and the resonant frequency gets higher. For  $F > 0.57$  (0.65) in the square (triangular) array, the stress from the almost still cylinders [the resonance is mainly concentrated in the matrix; see Fig. 3(d)] weakens the matrix's resonance, i.e., the Bragg scattering in the  $[1,1]$  direction becomes weaker, which leads to the narrower gap.

In conclusion, we have shown the resonance modes near the edges of the first absolute PBG in 2D PCs with a matrix of epoxy. The resonance of the gap top is induced by Bragg scattering, and the resonance is mainly concentrated in the matrix. The bottom resonance is induced by the joint effect of the Bragg and Mie scattering and presents a rotary resonance mode. The gap induced by the rigid-body resonance coalesces with the Bragg gap, so a wider gap comes into being. Then the physical understanding of the rotary resonance has been investigated by a simple model with an analytical solution. The behavior of this resonance has been characterized as a function of the mass densities of the cylinders. Finally, the effects of the array and the filling fraction on the first absolute phononic band gap are explained by the conditions for the occurrence of resonance.

The authors are grateful to Weimin Ye for valuable discussions. This work is supported by the State Key Development Program for Basic Research (Grant No. 51307) of China.

\*Email address: zhhg103@sina.com

<sup>1</sup>M. S. Kushwaha, P. Halevi, L. Dobrzynski, and B. Djafari-Rouhani, Phys. Rev. Lett. **71**, 2022 (1993).

<sup>2</sup>M. M. Sigalas and E. N. Economou, J. Sound Vib. **2**, 158377 (1992).

<sup>3</sup>E. Yablonovitch, Phys. Rev. Lett. **58**, 2059 (1987).

<sup>4</sup>J. O. Vasseur, P. A. Deymier, A. Khelif, Ph. Lambin, B. Djafari-Rouhani, L. Dobrzynski, A. Akjouj, L. Dobrzynski, N. Fettouhi, and J. Zemmouri, Phys. Rev. E **65**, 056608 (2002).

<sup>5</sup>J. O. Vasseur, P. A. Deymier, B. Chenni, B. Djafari-Rouhani, L.

- Dobrzynski, and D. Prevost, Phys. Rev. Lett. **86**, 3012 (2001).
- <sup>6</sup>M. Kafesaki and E. N. Economou, Phys. Rev. B **52**, 13 317 (1995).
- <sup>7</sup>R. Sainidou, N. Stefanou, and A. Modinos, Phys. Rev. B **66**, 212301 (2002).
- <sup>8</sup>K. Maslov, V. K. Kinra, and B. K. Henderson, Mech. Mater. **31**, 175 (1999).
- <sup>9</sup>Y. Cao, Z. Hou, and Y. Liu, Phys. Lett. A **327**, 247 (2004).
- <sup>10</sup>G. Wang, J. Wen, Y. Liu, and X. Wen, Phys. Rev. B **69**, 184302 (2004).
- <sup>11</sup>Z. Liu, X. Zhang, Y. Mao, Y. Y. Zhu, Z. Yang, C. T. Chan, and P. Sheng, Science **289**, 1734 (2000).
- <sup>12</sup>C. Goffaux and J. Sánchez-Dehesa, Phys. Rev. B **67**, 144301 (2003).
- <sup>13</sup>G. Wang, X. Wen, J. Wen, L. Shao, and Y. Liu, Phys. Rev. Lett. **93**, 154302 (2004).